

1 **Version of the attached file:** Peer reviewed preprint submitted to EarthArxiv₁

2 **Peer-reviewed status of the attached File:** peer reviewed₂

3 **Citation for the pre-print file:** Shaw, J.B., K.G. Mason, H. Ma, G. McCain (2021),
4 Influences on Discharge Partitioning on a Large River Delta: Case Study of the
5 Mississippi-Atchafalaya Diversion, 1926-1950

6 EarthArxiv: <https://osf.io/w3rxp>

7 **Additional information:** This manuscript is a preprint and has been submitted to
8 Water Resources Research for publication. The manuscript version posted on
9 EarthArxiv is non-peer reviewed and subsequent versions of the manuscript may
10 differ from this version. If the manuscript is accepted for publication, the final
11 typeset version will be available via the "Peer-reviewed Publication DOI" link on
12 The right hand side of this web page. Please feel free to contact any of the authors,
13 we welcome feedback.

14

15

16

17 **Influences on Discharge Partitioning on a Large River Delta: Case Study of the**
18 **Mississippi-Atchafalaya Diversion, 1926-1950**

19 **John B. Shaw¹, Kashauna G. Mason^{1,†}, Hongbo Ma^{1,*}, Gordon W. McCain III¹**

20 ¹Department of Geosciences, University of Arkansas, Fayetteville, AR, 72701

21 Corresponding author: John Shaw (shaw84@uark.edu)

22 [†]Currently at Department of Geology and Geophysics, Texas A&M University, College Station,
23 TX, 77843.

24 ^{*}Currently at Department of Environmental Sciences, University of Virginia, Charlottesville,
25 VA, 22904.

26 **Key Points:**

- 27 • The rapid increase in discharge to the Atchafalaya River between 1926 and 1950 is
28 explained first by natural erosion and second by dredging.
- 29 • Erosion measured in the lower Mississippi River would have reduced Atchafalaya
30 discharge had Atchafalaya Basin remained fixed.
- 31 • Delta growth in the Atchafalaya Basin did not change partitioning, as it was downstream
32 of a reach with steep water surface slope.
33

34 **Abstract**

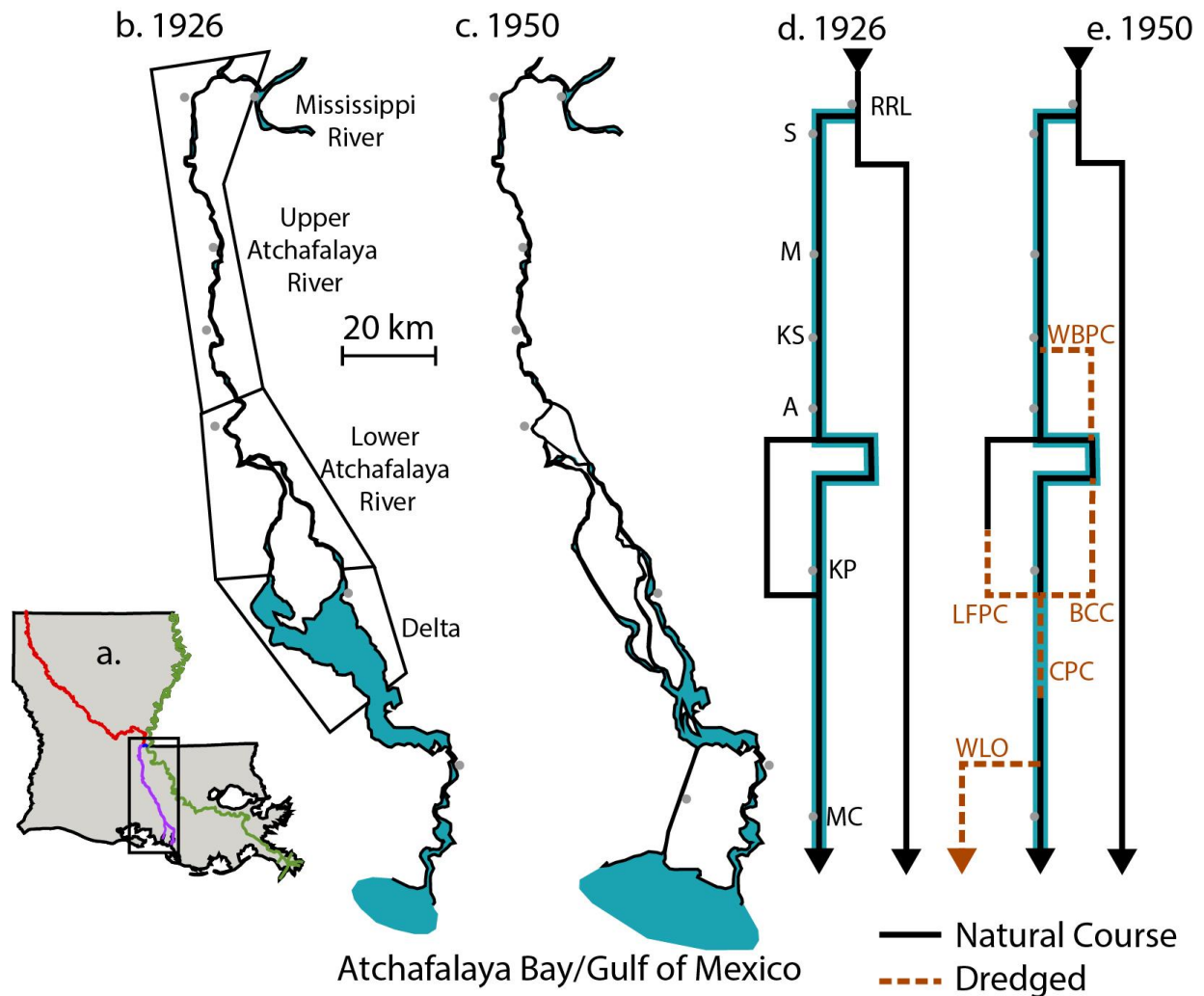
35 The modern Mississippi River Delta is plumed by the Mississippi and Atchafalaya rivers,
36 setting water and sediment dispersal pathways for Earth's fifth-largest river system. The
37 Atchafalaya River's (AR) partial annexation of discharge from the Mississippi River (MR),
38 particularly between 1926 and 1950, prompted warnings of a rapid river avulsion and the
39 construction of the Old River Control Structure to regulate flow. Natural and anthropogenic
40 causes of this discharge annexation are difficult to disentangle. Here, we develop and validate a
41 hydrodynamic model of flow partitioning through the historic channel network. We then isolate
42 how several key changes to the system affected discharge partitioning and stage at the AR-MR
43 diversion. Simulations show that erosion of the upper AR can account for 73% of the water
44 discharge increase. Dredging in the lower AR between 1932 and 1950 can account for 35% of
45 the water discharge increase, and was also an important control on shear stress distribution. The
46 lower MR was slightly erosional during this period, and therefore hindered the AR discharge
47 increase. Significant lacustrine delta deposition in AR had little effect on partitioning. These
48 findings highlight the importance of AR enlargement processes on avulsion dynamics at this site.
49 Given the essential nature of this river junction to the society, transportation, and commerce of
50 the United States, improved attribution of discharge increases may lead to future management
51 strategies that are broadly impactful.

52

53

54 **1 Introduction**

55 Many of the world's large river deltas evolve under a combination of natural and human forcings
56 (Ganti et al., 2014; Kleinhans et al., 2011; Vinh et al., 2014; Wilson et al., 2017). However,
57 frameworks for attributing change among several forcings that occur simultaneously remain
58 elusive. The problem is further compounded by the complexity of many river deltas, where
59 forcings interact non-locally through a network of many distributary channels (Bain et al., 2019;
60 Kästner et al., 2017; Kleinhans, Ferguson, et al., 2012). Constraining these interactions is essential
61 for the many large-scale management and engineering initiatives that will significantly alter
62 modern deltas to optimize for their sustainable future (Hoitink et al., 2020; Syvitski, 2008; Tessler
63 et al., 2015). Here, we study the influence of several natural and human-induced influences on
64 historic discharge annexation in the complex channel network of the Mississippi Delta System.

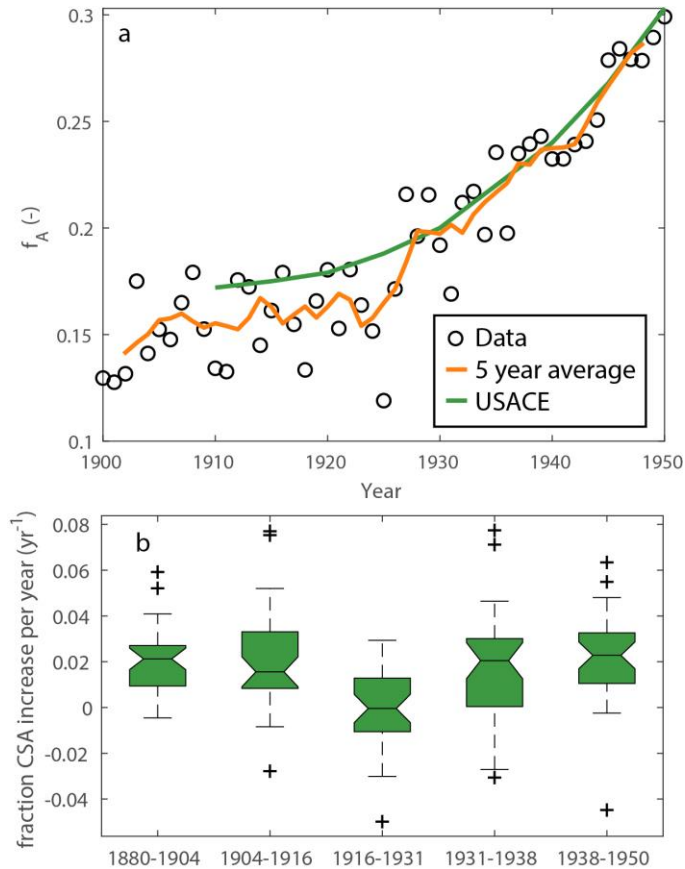


65

66 **Figure 1.** (a) Map of Louisiana showing the Mississippi River (green), Atchafalaya River
 67 (purple), and Red River (red). (b and c) Maps of Atchafalaya River in 1926 and 1950, with
 68 Mississippi course removed for clarity. Gray circles are hydrograph stations. Polygons (in
 69 b) show different regions referred to in the text. (d and e) Model schematics for flow
 70 routing. Arrow tails show flow sources and arrow heads show sinks at sea level. The
 71 pathway which is plotted in Figs 5a,c and 6 is outlined in blue. RRL: Red River Landing,
 72 S: Simmesport, M: Melville, KS: Krotz Springs, A: Atchafalaya, KP: Keelboat Pass, MC:
 73 Morgan City, WBPC: Whiskey Bay Pilot Channel, BCC: Bayou Chene Cutoff, CPC:
 74 Chicot Pass Channel, LFPC: Lake Fausse Point Channel, WLO: Wax Lake Outlet.

75 The modern Mississippi Delta system (Figure 1) is the product of natural processes across geologic
 76 time (Blum, 2019; Saucier, 1994). Over the Holocene, the Mississippi River delta has experienced
 77 semi-periodic avulsions, or the rapid abandonment of a channel course for a new course through
 78 the delta (Blum & Roberts, 2012; Fisk, 1952; Saucier, 1994). The Atchafalaya River is the most
 79 recent new course. It was initiated in the sixteenth century, and was well-established in 1765 (Fisk,
 80 1952).

81 Human activities began to significantly change the system's morphology and hydrology in the
 82 nineteenth century (Kesel, 2003; Mossa, 2013). These included dredged meander cutoffs that
 83 straightened the Mississippi River's course (1831-1942) and large log jams that were removed
 84 from the Atchafalaya River (1839-1855; Mossa, 2013). At Red River Landing (Fig. 1), where the
 85 Old River (an abandoned meander loop) connects the Mississippi and Atchafalaya rivers, a canal
 86 was dredged intermittently between 1878 and 1937 to maintain navigable low-water connection
 87 between the rivers (Fisk, 1952; Mossa, 2013). Between 1900 and 1932, the Atchafalaya River
 88 flowed into the Mississippi River an average of 37 days per year, with the last flow in this direction
 89 in 1945 (Latimer and Schweizer 1951; their Table 36).



90
 91 **Figure 2.** (a) Time series of the proportion of mean annual discharge entering the Atchafalaya
 92 River from the Mississippi River f_A . Orange line is a five-year moving average. Green line is
 93 the USACE's interpreted f_A trajectory. (b) Distribution of change in upper Atchafalaya River
 94 bank-full cross-sectional area (CSA) for $n=35$ transects across five time periods (compiled
 95 by McCain, 2016; $0.02 = 2\%$ average increase per year). Transects were surveyed by USACE
 96 in the 66 km of Atchafalaya River downstream of the Red River (See Fig. 1). Notched box
 97 plots (Kafadar, 2014) with whiskers showing one IQR above and below box. Plus signs show
 98 outliers. Line is median. Notch is the 95% confidence interval of the median
 99 ($\pm 1.571\text{IQR}/\sqrt{n}$). The period 1916-1931 shows statistically smaller increases than the other
 100 periods (notches do not overlap).

101 USACE measurements of the fraction of annual water discharge leaving the Mississippi River and
 102 entering the Atchafalaya River (f_A) show a period of relative discharge stability from 1900-1925

103 and a period of discharge annexation with rapidly increasing f_A beginning in 1926 (Figure 2a).
104 During the stable phase, f_A was larger during years with more discharge, but no temporal trend is
105 apparent. After 1926, f_A increased at a roughly linear rate of 0.005 yr^{-1} until 1950. This period of
106 annexation is the focus of our study.

107 The increase in f_A was interpreted widely as the gradual and inevitable annexation of flow from
108 the established Mississippi channel to produce a new avulsion through the Atchafalaya basin
109 (green line, figure 2a). The discharge annexation (increasing f_A) was attributed to the gradient
110 advantage of the Atchafalaya River relative to the existing Mississippi channel (240 km vs 496
111 km), that was thought to increase scouring in the Atchafalaya River (Fisk, 1952; Latimer &
112 Schweitzer, 1951). The diversion angle and partitioning of sediment discharge were considered to
113 have a secondary effect on the discharge increase. By extrapolating the rates of discharge
114 partitioning increase and channel enlargement using an unpublished Army Corps internal report
115 by Graves, it was estimated that the Atchafalaya River would annex 40% percent of the
116 Mississippi's discharge between 1965 and 1975, after which the predicted avulsion would be rapid
117 and unstoppable (Fisk, 1952; Latimer & Schweitzer, 1951). The apparent inevitability of avulsion
118 caused the Old River Control Structure (ORCS) to be built in 1963, to regulate f_A . The "Control of
119 Nature" exerted by ORCS reached the public consciousness through the famous essay by McPhee
120 (1987).

121 The processes that controlled the rapid increase in f_A are important, and have received insufficient
122 attention. River avulsions control sedimentary basin filling, and the Mississippi-Atchafalaya
123 system is considered an important modern analogue (Bhattacharya et al., 2019). Furthermore,
124 sustainable management of modern river deltas subjected to rapid relative sea level rise requires a
125 clear understanding of how natural and anthropogenic processes influence water, sediment, and
126 nutrient transport pathways (Knights et al., 2020; Sanks et al., 2020). The USACE analyses (Fisk,
127 1952; Latimer & Schweitzer, 1951) were based on empirical analyses of extensive datasets.
128 However, a quantitative analysis of the historic system's hydrodynamics has yet to be performed.
129 This is partly because hydrodynamic models were still in their infancy in the early 1950s (e.g.
130 Chow, 1959). Since then, the understanding of avulsion has advanced significantly (Kleinhans,
131 Ferguson, et al., 2012; Slingerland & Smith, 2004; Z. B. Wang et al., 1995), yet modeling of
132 specific avulsions continues to be rare. Hence, we found it compelling to revisit this problem with
133 physics based models that could quantitatively analyze discharge partitioning based on historic
134 measurements, in order to lessen uncertainties and uncover controls of this essential river
135 junction's evolution.

136 1.1 Factors Potentially Influencing Partitioning

137 We examine a hydrodynamic model of water discharge through the historic Mississippi-
138 Atchafalaya network (Figure 1) to quantitatively assess controls on the rapid increase in
139 Atchafalaya River discharge (Figure 2). We isolate four potential controls: (i) the widening of the
140 Upper Atchafalaya River, (ii) evolution of the lower Mississippi River, (iii) the dredging of
141 channels in Lower Atchafalaya River, and (iv) the progradation of lacustrine deltas into the lakes
142 of the lower Atchafalaya Basin.

143 The natural widening and incision (termed hereafter "natural erosion") of the upper Atchafalaya
144 River between Red River Landing and the Atchafalaya, LA gauge (100 km downstream of Red
145 River Landing; Fig. 1, 2b) has been interpreted as the key influence of increasing f_A (Fisk, 1952).

146 Surveys by Latimer and Schweitzer (1951) show that enlargement of bank-full cross-sectional area
147 was a relatively consistent between 1880 and 1950 (median growth $0.016\text{-}0.022\text{ yr}^{-1}$; i.e. 1.6-2.2%
148 increase in bank-full cross-sectional area per year), except 1916-1931 which was remarkably slow
149 (median $-0.0004 \pm 0.0062\text{ yr}^{-1}$; Fig. 2b). Erosion in this region may have been facilitated by a
150 substrate of sand bodies from the historic Mississippi River that were easily erodible (Aslan et al.,
151 2005). The associated increase in cross-sectional area should lead to increased f_A .

152 The lower Mississippi river was also evolving in the early 20th century. Kesel's (2003) analysis
153 of Mississippi River hydrographic surveys downstream of Red River Landing suggested erosion
154 of the channel thalweg between 1935 and 1948, and interpreted it as the result of a river
155 straightened and steepened by meander cutoffs. Stage-discharge relationships on the Mississippi
156 River between Arkansas City, AR and Red River Landing showed similar reductions in stage for
157 a given discharge between 1930 and about 1945 before increasing gradually after 1945
158 (Biedenharn & Watson, 1997; Smith & Winkley, 1996). Our analysis of the 1916 and 1949
159 hydrographic surveys shows that channel thalweg (minimum elevation) did not change
160 significantly, but the cross-sectional area of flow grew slightly, particularly in the final 200 km
161 of the Mississippi River (downstream of New Orleans, LA). See section 4.1 for discussion. Such
162 an increase in Mississippi River cross-sectional area should lead to decreased f_A .

163
164 Between 1932 and 1951, $97 \times 10^6\text{ m}^3$ of sediment was dredged from the Atchafalaya River Basin
165 (Latimer and Schweitzer, 1951). While the USACE reports mention dredging activities within the
166 Atchafalaya Basin, they were not considered a significant factor controlling the discharge
167 partitioning (Fisk, 1952), possibly because the dredging was focused in lower Atchafalaya River
168 and Deltas region (Fig. 1b), $>100\text{ km}$ from Red River Landing. Dredging consisted of navigation
169 channels that did not previously exist, including the Whiskey Bay Pilot Channel (WBPC), the
170 Bayou Chene Cutoff (BCC), and the Chicot Pass Channel (CPC) and the Wax Lake Outlet (WLO;
171 Fig. 1). Channels were dredged to 4.5-6.1 m (15-20 feet) deep and 90 m (300 feet) wide. Channels
172 dredged early in this period sometimes deepened and widened considerably between dredging and
173 the USACE survey of 1950 (Figure 3). This dredging could also increase f_A .

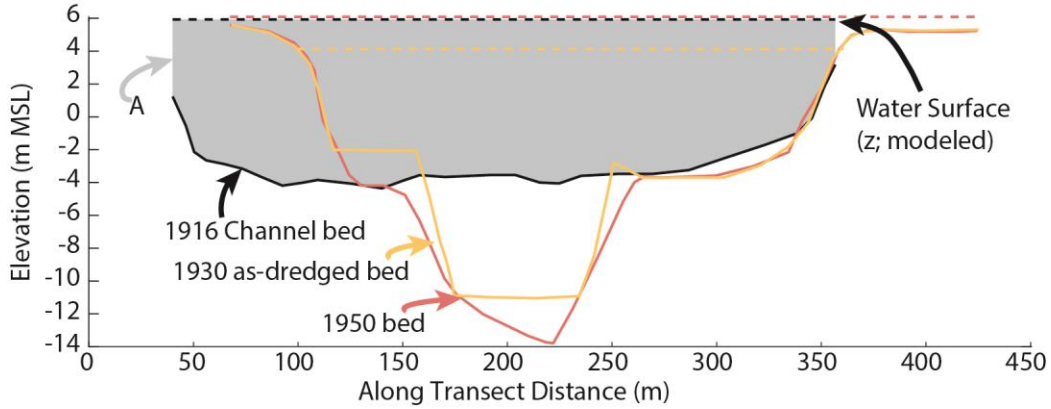
174 The fourth change to the system that could influence f_A is the growth of the large deltas in Grand
175 Lake in the Atchafalaya Basin ("Deltas" Region, Figure 1b). Between 1916 and 1950, about 180
176 km^2 of lacustrine delta deposits accumulated, largely filling the $\sim 3\text{ m}$ deep Grand Lake (Roberts
177 et al., 1980; Tye & Coleman, 1989). While natural channels formed during this accumulation,
178 channelization was dominated by the dredged Chicot Pass Channel (Figure 1e). Such deposits
179 could have acted to reduce cross sectional area of flow, causing a reduced discharge for the same
180 water surface slope in the Atchafalaya Basin, thereby decreasing f_A .

181 **2 Model and Data**

182 We construct a numerical model of steady, non-uniform flow through a complex channel
183 network. The model is an adaptation of 1-Dimensional flow models (Chow, 1959; Parker, 2004)
184 that have proven effective for tracking discharge and fluid shear stress for single-channel coastal
185 rivers (Chadwick et al., 2019; Lamb et al., 2012; Nittrouer et al., 2012; Viparelli et al., 2015).
186 We advance this approach by including channel bifurcations and confluences in order to resolve
187 discharge partitioning. Discharge partitioning has been studied for an ideal branch (Buschman et
188 al., 2010; Slingerland & Smith, 1998; Z. B. Wang et al., 1995) and in the case of a complex
189 network (Kleinmans, de Haas, et al., 2012). Our work considers controls on discharge partitioning

190 as a function of documented changes to channel and network morphology for the first time.
 191 Using bathymetric transects and stage-discharge relationships from before the discharge
 192 annexation (Figure 2), we validate a hydrologic model of the system. We then isolate the
 193 influence of key changes to the system by constructing synthetic networks, and assess controls
 194 on discharge partitioning.

195 2.1 Model



196

197 **Figure 3.** Diagram of cross section R-143, in the Atchafalaya Basin. Black, yellow, and
 198 red solid lines signify the 1916 transect used in R_{pre} , the 1930 transect with the planned
 199 dredging used in R_{pre_D} , and the 1950 transect after additional erosion used in R_{post} .
 200 Dashed lines show example modeled water surface elevations. The gray region is an
 201 example of cross-sectional area A for the R_{pre} .

202 We begin with one-dimensional expressions for conservation of fluid mass and conservation of
 203 fluid momentum:

$$204 \quad \frac{\partial A}{\partial t} + \frac{\partial Q}{\partial x} = 0, \quad (1)$$

$$205 \quad \frac{\partial Q}{\partial t} + \frac{\partial(Q_i^2/A)}{\partial x} = gA \left(-\frac{\partial z}{\partial x} - S_f \right), \quad (2)$$

206 where t is time [T]; x is streamwise spatial distance [L]; g is gravitational acceleration [LT^{-2}]; A
 207 is the wetted cross-sectional area [L^2] (Figure 3); Q_i is the water discharge [L^3T^{-1}] through reach
 208 i ; z is the water surface elevation; $S_f = C_f u |u| / (gA / \Gamma)$ is the frictional slope where C_f is the
 209 resistance coefficient [-], u is the cross-sectionally averaged velocity $u = Q / A$ [LT^{-1}], and Γ is
 210 the wetted perimeter, or A divided by the wetted surface width [L]. Under steady conditions $\partial/\partial t$
 211 ≈ 0 , Eqs. (1-2) reduce to

$$212 \quad \frac{\partial z}{\partial x} = -\frac{1}{gA} \frac{\partial(Q_i^2/A)}{\partial x} - S_f. \quad (3)$$

213 For a known bathymetric transect (Figure 3), A and Γ can be calculated as a function of z *a*
 214 *priori*: we do so in 0.1 m increments for z between 0 and 25 m above sea level for all transects.
 215 With prescribed Q_i and C_f and known z at a downstream transect, equation (3) can be solved

216 directly without further assumptions of channel width or depth, allowing the water surface to be
 217 solved for the upstream transect.

218 We now extend this framework to model a network of many interacting channel reaches. In order
 219 to solve for A , u , and Q throughout the channel network, it is broken into non-branching reaches i
 220 joined at nodes representing bifurcations and confluences. Under Froude-subcritical conditions (F^2
 221 < 1), the boundary conditions Q_i and the downstream water depth allow Eq. 3 to be solved along
 222 each reach. Reaches are linked by discharge constraints. At a node where an upstream channel a
 223 bifurcates into two channels b and c , we specify $Q_a = Q_b + Q_c$, with the discharge partitioning
 224 fraction defined as $f_b = Q_b/Q_a$. At a confluence node where two channels d and e flow together to
 225 form a single channel f , $Q_d + Q_e = Q_f$. Although upstream flow ($Q_i < 0$) is potentially possible in
 226 some networks, we stipulate $Q_i \geq 0$ in this study because tidally averaged flows are always
 227 unidirectional through this system.

228 Two hydraulic boundary conditions are required for a model run (beyond the bathymetric transects
 229 summarized in Section 2.2). First, upstream discharge (Q_0) is specified at the Mississippi River at
 230 Red River Landing (RRL; Fig. 1). The Red River also provides discharge to the system, and can
 231 be as large as 10% of the Mississippi River's discharge. However, we do not model it here because
 232 it enters the Atchafalaya River upstream of Simmesport, where Atchafalaya River discharge and
 233 f_A is measured by Latimer and Schweitzer (1951). Second, the boundary condition of water surface
 234 elevation is applied at each channel terminus ($z = 0$ m MSL; at the Mississippi River mouth, the
 235 Atchafalaya River mouth, and the Wax Lake Outlet mouth in pertinent models). This terminus was
 236 chosen where significant tributary outflow began to occur, consistent with Lamb et al. (2012).

237 The model is solved by finding discharge partitioning values f_i that minimize differences in water
 238 surface elevation at each bifurcation in the network (Fig. 1d,e). (1) An initial set of arbitrarily
 239 chosen discharge partitionings f_{i0} for every channel bifurcation (including the Mississippi-
 240 Atchafalaya bifurcation) is assumed (f_A set to 0.3); (2) based on f_{i0} , the discharge within each reach
 241 is computed by integrating equation (3) upstream from channel mouths at the Atchafalaya River,
 242 Mississippi River, and Wax Lake Outlet in some cases (Fig. 1d,e); (3) at each bifurcation, the
 243 water surface elevation at the downstream end of the upstream reach (z_{0a}) is set equal to the water
 244 surface elevation at the upstream end of one of the reaches b or c (z_{1b} , z_{1c}); (4) when flow has been
 245 solved throughout the network, the sum of squared difference in water surface elevation at each
 246 channel bifurcation $E = \sum \Delta z^2 = \sum (z_{1b} - z_{1c})^2$ is iteratively minimized using the quasi-newton
 247 optimization technique found in MATLAB (Shanno, 1970) to alter partitionings f_i . When a
 248 minimum of E is found, each bifurcation will have a nearly equal water surface elevation ($z_{0a} \approx z_{1b}$
 249 $\approx z_{1c}$) and the water surface will be nearly continuous throughout the channel network. For model
 250 runs described here, final solutions of f_i produce very small absolute water differences ($E < 10^{-6}$
 251 m^2) ensuring near-continuity state of the water surface across the network, and a plausible
 252 reconstruction of fluid flow.

253 2.2 Hydrographic Survey Data and Network Models

254 This study relies on detailed bathymetric and hydrological measurements collected by the US
 255 Army Corps of Engineers that are used to calculate A and Γ (Figure 3). We digitized these
 256 measurements from original documents and a library of these hydrographic surveys and models
 257 are included in the supplementary material.

258 The pre-annexation model (R_{pre}) consisted of the most recent surveys prior to significant
259 discharge annexation. This model contained five reaches (Fig. 1d), with bifurcations at Red River
260 Landing (RRL) and within the lower Atchafalaya River. Minor channels and over-marsh flow were
261 neglected. The Atchafalaya River portion of this model consisted of hydrographic surveys
262 collected between 1910 and 1926 published in Latimer and Schweitzer (1951, Vol. 3). The mean
263 transect spacing was 3.5 km. The Mississippi River portion of the model was the 1913 Mississippi
264 River Hydrographic Survey (USACE, 1915) between the Mississippi-Atchafalaya Bifurcation
265 near Red River Landing, and Venice, LA, where significant flow begins leaving the main channel,
266 17 km upstream of head of passes. The mean transect spacing was 0.3 km.

267 The post-annexation model (R_{post}) consisted of hydrographic surveys collected near the end of
268 significant dredging in 1950. This model contained 11 reaches (Fig. 1e) with five bifurcations. The
269 additional bifurcations relative to R_{pre} were due to the Whiskey Bay Pilot Channel, Bayou Chene
270 Cutoff, and Wax Lake Outlet. Minor channel and over-marsh flows were neglected. Dredging from
271 the Lake Fausse Pointe Cut and Atchafalaya Basin Main Channel altered existing transects. These
272 Atchafalaya River surveys are also published in Latimer and Schweitzer (1951, Vol. 3). The
273 Mississippi River portion of this model was the 1949 Mississippi River Hydrographic Survey
274 (USACE, 1950) between Old River and Venice.

275 Stage-discharge relationships were recorded at seven locations, from Red River Landing (at the
276 junction of the Mississippi and Atchafalaya Rivers) to Morgan City, Louisiana (Fig. 1b,d; Latimer
277 and Schweitzer, 1951). Such relationships were recorded in 1880 and then every few years from
278 1935-1950. The relationship from 1935 served as a pre-annexation validation, and the relationship
279 from about 1950 served as the post-annexation comparison.

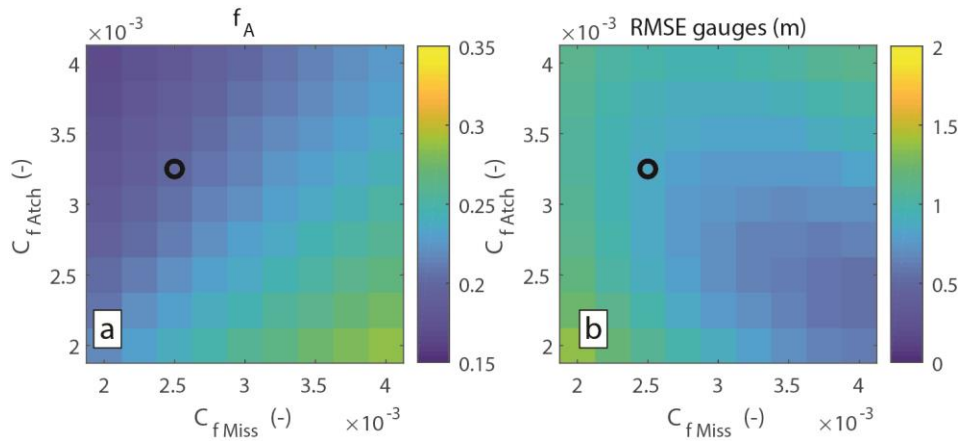
280 To isolate the effects of key changes within the basin, several synthetic hydrodynamic models
281 were constructed that altered certain aspects of Model R_{pre} (Table 1). Model R_{pre_A} isolated
282 the effect of channel widening in the Atchafalaya Basin by taking the R_{pre} model and exchanging
283 the 1950 cross sections of the Upper Atchafalaya River where channel area had significantly
284 increased. Model R_{pre_D} isolated the effect of dredging in the Atchafalaya River by exchanging
285 bathymetric transects from R_{pre} with planned dredging cross sections (i.e. Fig. 3), including the
286 newly dredged channels such as Whiskey Bay Pilot Channel (WBPC; Fig. 1e). Model R_{pre_M}
287 isolated the influence of changes in the Mississippi River over the study period by taking the R_{pre}
288 model and exchanging the 1949 Mississippi River hydrographic survey. Finally, Model R_{pre_GL}
289 isolated the effect of sediment accumulation within Grand Lake by taking model R_{pre} and
290 exchanging R_{post} transects only within the Deltas Region (Fig. 1).

291 **3. Results**

292 **3.1 Validation**

293 The R_{pre} hydrodynamic model was validated against (a) the measured discharge partitioning
294 (five year average $f_A = 0.17$; Fig. 2) and (b) measured stage-discharge curves. An upstream
295 discharge of $Q_0 = 18,300 \text{ m}^3/\text{s}$ was used throughout the validation and modeling process because
296 it is the Mississippi River's average annual discharge between 1900 and 1960 (Latimer and
297 Schweitzer, 1951). Preliminary simulations were run with discharges ranging from 15,000-35,000
298 m^3/s which showed gradually increasing f_A with increasing Q_0 , consistent with Edmonds (2012).

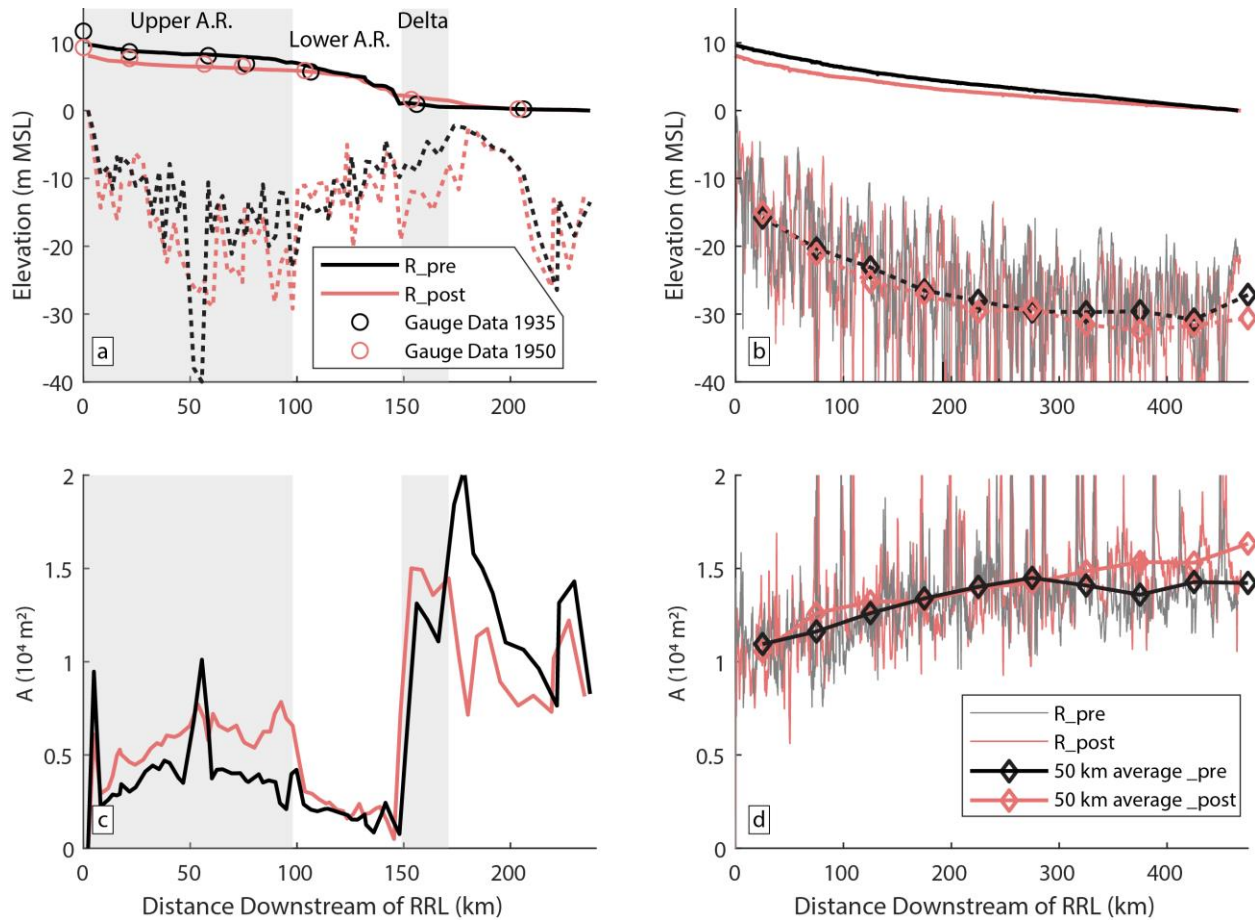
299 However, our focus on the recorded increase in average annual flows to the Atchafalaya River
 300 meant that we left detailed simulation of variable discharge through the system to future work.



301

302 **Figure 4.** (a) modeled partitioning of flow before annexation and (b) root-mean-square error of the
 303 7 stage-discharge gauges were used to determine an ideal combination of friction factor (C_f) in the
 304 Mississippi River (x axes) and Atchafalaya River (y axes). The black circles show the friction
 305 factors that were chosen for modeling. Results shown for upstream discharge $Q_0 = 18,300 \text{ m}^3/\text{s}$.

306 Model R_pre was run for a variety of friction factors in both the Mississippi River (C_{f_Miss}) and
 307 the Atchafalaya network (C_{f_Atch}) ranging from 0.001 and 0.004 (Figure 4). Partitioning (f_A)
 308 increased with increasing C_{f_Atch} and decreasing C_{f_Miss} . We chose $C_{f_Atch} = 0.00325$ and $C_{f_Miss} =$
 309 0.0025 for this study, as it produced a reasonable value of f_A (0.199) based on the field data, and a
 310 reasonably small value of RMSE (0.865 m), just 5% of the 18 m average flow depth. These values
 311 of C_f are consistent with the direct measurement at Tarbert Landing, Mississippi River (Karim,
 312 1995) and the prediction of the prevailing resistance relation (Engelund & Hansen, 1967). This is
 313 consistent with friction factors used to model the modern Mississippi river by Nittrouer et al.
 314 (2012; 0.003 - 0.007), and by Edmonds (2012; 0.0023).



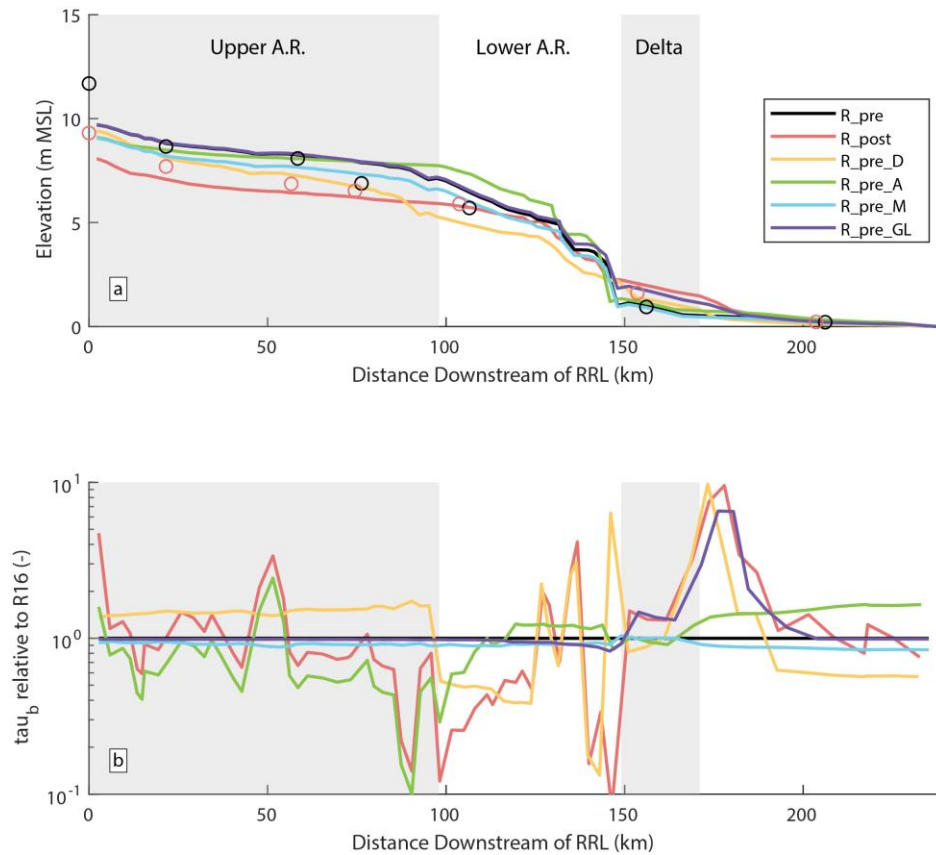
315

316 **Figure 5.** Results for models R_pre (black) and R_post (red) for upstream discharge $Q_0 =$
 317 $18,300 \text{ m}^3/\text{s}$, with $f_A = 0.199$. Panels a (thalweg elevation dotted, and water surface solid)
 318 and c (cross-sectional area A) show the primary path through the Atchafalaya River
 319 network (see Fig. 1d,e). Panels b and d show the lower Mississippi River, with transect
 320 data and 50 km averages. In (a), circles indicate hydrograph elevation for the modeled Q
 321 collected before (1935) and after (1950) significant discharge annexation.

322

323 Using these C_f values, discharge partitioning (f_A) between the Mississippi and Atchafalaya Rivers
 324 was simulated for $Q_0 = 18,300 \text{ m}^3/\text{s}$ for each model of the Mississippi-Atchafalaya system. For
 325 models R_pre and R_post (the pre- and post-annexation models), f_A was 0.199 and 0.278,
 326 respectively. These results compare well with data showing f_A of 0.17 in 1926 and 0.29 in 1950.
 327 Model runs R_pre and R_post and measured stage-discharge relationships (Figure 5a, Table 1)
 328 show a similar water surface profile for average annual discharge to the system. The large, low-
 329 slope channel in the upper Atchafalaya River transitions to the smaller A , higher-slope channel in
 330 the lower Atchafalaya River, producing a concave down “M2 curve” (Chow, 1959) from 110-130
 331 km downstream of Red River Landing (Figure 5a, b). At the transition to the wide and shallow
 332 Grand Lake, slopes are significantly reduced again, producing a concave up “M1 curve”.

333 The post-annexation model (R_post) and data differ from their pre-annexation counterparts
 334 (R_pre) in terms of their water surface slopes in the upper Atchafalaya River (for the same Q_0 , but
 335 37% increase in Q in the Atchafalaya River; Table 1). Hydrograph data show that the stage at Red
 336 River Landing dropped 2.4 m, consistent with the modeled 1.6 m drop. Relatedly, slopes in the
 337 upper Atchafalaya River (measured over 104 km between RRL and Atchafalaya, LA) dropped
 338 30% in the hydrograph data and 15% between R_pre and R_post.



339

340 **Figure 6.** (a) Water surface profiles along the primary pathway through the Atchafalaya
 341 Basin (see Fig. 1) for all models (see Table 1). Black and red circles are water stages
 342 estimated from stage discharge measurements in 1935 (R_pre) and 1950 (R_post),
 343 respectively. (b) Fluid shear stress ($\tau_b = \rho C_f u^2$) along each transect divided by the shear
 344 stress from run R_pre. Note logarithmic y axis.

345

346 3.2 Partitioning Attribution

347 Synthetic channel networks of the Mississippi-Atchafalaya System (described in Section 2.2) were
 348 used to test how various changes during the period of discharge annexation influenced discharge
 349 partitioning (Figure 6, Table 1). Several important aspects of the simulations are considered here.
 350 First, model f_A is compared to the results from R_pre and R_post (f_A of 0.199 and 0.278
 351 respectively) in order to assess the control on discharge partitioning. Second, the stage change at
 352 Red River Landing is compared to the simulated stages (9.7 m and 8.1 m respectively). Finally,

353 the fluid shear stress ($\tau_b = \rho C_f u^2$) in the upper Atchafalaya River, a proxy for sediment transport
 354 and erosion potential, is analyzed relative to the R_pre baseline (Fig. 6b).

355 When the natural erosion of the Atchafalaya River was isolated (Model R_pre_A), f_A increased to
 356 0.257, or 73% of the required discharge increase from R_pre to R_post. The stage at RRL dropped
 357 to 9.1 m, explaining only 40% of the total stage drop. However, the average shear stress in the
 358 upper Atchafalaya River decreased, as increased cross-sectional area led to reduced water
 359 velocities.

360 The isolated effects of dredging (Model R_pre_D) produced a partitioning of $f_A = 0.227$, explaining
 361 35% of the modeled change between R_pre and R_post. The stage at RRL dropped to 9.4 m, only
 362 19% of the total stage change there. Change was focused where dredging of new channels occurred
 363 in the lower Atchafalaya River (Figure 1, 6), but this led to increased water surface slopes and a
 364 44% fluid shear stress increase in the upper Atchafalaya River.

365 The isolated effects of Mississippi River erosion (Model R_pre_M) showed $f_A = 0.183$, the only
 366 model that significantly reduced f_A relative to R_pre. This is because minor increases to channel
 367 cross-sectional area of the Mississippi River (and no change in the Atchafalaya River in this
 368 synthetic model) acted to reduce slopes in the Mississippi River and stage at RRL to 9.0 m, thereby
 369 reducing discharge to the Atchafalaya River. The stage reduction was 44% of the total reduction
 370 in stage between R_pre and R_post. Fluid shear stress in the Atchafalaya River was minimally
 371 affected.

372 Despite the growth of significant lacustrine delta deposits between 1916 and 1950, the isolated
 373 effects of lacustrine deltas progradation (Model R_pre_GL) produced essentially the same
 374 discharge partitioning and RRL stage as R_pre. This suggests that they had little to no impact on
 375 the discharge partitioning at the Mississippi-Atchafalaya bifurcation.

376 **Table 1.** Hydrograph data and hydrodynamic model outputs for the Mississippi-Atchafalaya
 377 system. Models R_pre and R_post simulate the system before and after the discharge annexation
 378 between 1926 and 1950 (see Figure 2). Model R_pre_A isolates natural erosion in the upper
 379 Atchafalaya River, R_pre_D isolates the contribution dredging in the Atchafalaya Basin, Model
 380 R_pre_M isolates lower Mississippi River evolution, and Model R_pre_GL isolates deposition in
 381 Grand Lake.

	f_A (-) ($Q_0=18,300$ m^3/s)	Upper A.R. Water Surface Slope ($\times 10^{-5}$)	Lower A.R. Water Surface Slope ($\times 10^{-5}$)	z at RRL (m MSL)	Fraction of f_A change explained by model	Mean τ_b , Upper A.R. (N/m^2)
Data 1926	0.17	5.7	10.0	11.7	N/A	
Data 1950	0.29	4.0	9.1	9.3	N/A	
R_pre	0.199	2.6	11.9	9.7	N/A	3.6

R_post	0.278	2.2	7.2	8.1	N/A	2.9
R_pre_A	0.257	1.4	12.8	9.1	73%	2.0
R_pre_D	0.227	4.1	6.0	9.4	35%	5.2
R_pre_M	0.183	2.5	11.0	9.0	-20%	3.3
R_pre_GL	0.198	2.6	10.3	9.7	-1%	3.6

382

383 4 Discussion

384 4.1 Attribution to the Atchafalaya partial avulsion

385 The numerical model described here quantitatively reproduces the increase in the proportion of
 386 discharge down the Atchafalaya River over the period of discharge annexation (Figures 4, 5).
 387 The non-linearity of the hydrodynamic model prevents attribution from neatly summing to
 388 100%, but analysis of synthetic models clearly shows that it can be attributed to several
 389 simultaneous processes. The increase in cross-sectional area of the Upper Atchafalaya River due
 390 to natural erosion (shown in R_pre_A) produced the largest increase in f_A (Table 1). This is
 391 consistent with the original assessment of the Army Corps of Engineers (Fisk, 1952). However,
 392 previously unexamined factors also influenced the system, including dredging in the Atchafalaya
 393 River and erosion in the Mississippi River. The significant lacustrine delta deposition did not.

394 The increase of cross-sectional area in some parts of the lower Mississippi River between 1913
 395 and 1951 (the years of the USACE surveys) has not been previously linked to the Mississippi-
 396 Atchafalaya diversion. We attribute 42% of the 1.9 m stage reduction at Red River Landing to
 397 lower Mississippi River changes (Table 1). The increase in cross-sectional area occurred in two
 398 locations. First, 50-150 km downstream of Red River Landing (roughly between St. Francisville
 399 and Plaquemine, LA) in the fully alluvial reach of the river, and >300 km downstream
 400 (downstream of New Orleans, LA; Figure 5) in the alluvial-bedrock reach of the river (Viparelli
 401 et al., 2015). While reach-averaged increases to cross-sectional area were between 5 and 15%
 402 (diamonds Fig. 5d), they impacted f_A by reducing water surface slopes in the Mississippi River,
 403 and therefore the stage at Red River Landing. Lower Mississippi River erosion during the period
 404 of discharge annexation by the Atchafalaya River is consistent with previous studies (Kesel,
 405 2003; Smith & Winkley, 1996). However, it is worth noting that since this period, the lower
 406 Mississippi River has had periods of both aggradation and degradation (Galler et al., 2003; Knox
 407 & Latrubesse, 2016; B. Wang & Xu, 2016, 2018; Wu & Mossa, 2019). Had the lower
 408 Mississippi River been aggradational during the study period, f_A would likely have increased
 409 more rapidly.

410 There are remarkable differences in hydrodynamics for models isolating the natural erosion
 411 (R_pre_A) and dredging (R_pre_D) models of the Atchafalaya River (Fig. 6). When natural
 412 erosion is considered in the absence of dredging, discharge increases can only be accommodated
 413 by increased slopes in the lower Atchafalaya River (R_pre: 11.9×10^{-5} , R_pre_A 12.8×10^{-5}) which
 414 produce higher stages and lower slopes in the upper Atchafalaya River (Fig. 6a). In contrast,

415 when dredging is considered in the absence of natural erosion (R_pre_D), reduced slopes in the
416 lower Atchafalaya River are possible (R_pre_D: 6.0×10^{-5}), which lead to reduced stages and
417 higher slopes in the upper Atchafalaya River.

418 The effects on fluid shear stress ($\tau_b = \rho C_f u^2$) in the upper Atchafalaya River are remarkable
419 (Fig. 6b). Shear stress is reduced by 44% due to natural erosion (3.6 to 2.0 N/m²; R_pre_A;
420 Table 1) despite a 29% discharge increase down the Atchafalaya River ($Q_0 = 18,300$ m³/s held
421 constant). In contrast, the 14% discharge increase of R_pre_D increases shear stress by 44% (3.6
422 to 5.2 N/m²). Hydrograph data offer a consistent story. Between 1932 and 1950 (dates of data
423 collection), the water surface slope decreased 30% (5.7×10^{-5} to 4.0×10^{-5} ; Figure 6a) in the
424 upper Atchafalaya River but decreased only 9% in the lower Atchafalaya. The erosion of the
425 upper Atchafalaya River is presumably the result of heightened shear stresses, and the period of
426 dredging (1932-1951) showed consistently large rates of cross-sectional area increase (Fig. 2b).
427 Our results show that a negative feedback between cross-sectional area increase and shear stress
428 in the upper Atchafalaya River could limit further erosion, but increased channelization in the
429 lower Atchafalaya due to dredging could remove this feedback and potentially lead to greater
430 erosion.

431 **4.2 Limitations and Advantages**

432 The model considered here were constructed in a manner so that they could be adequately run
433 with the available historic data and allow several hypotheses to be tested. While the present study
434 compares well with validation data and produces first order attribution, more complex models
435 are necessary to include sediment transport, bed evolution, or the investigation of particular
436 floods. Globally, coastal systems are evolving under simultaneously active natural and human
437 drivers (Hoitink et al., 2020; Lazarus & Goldstein, 2019). The methods presented here are
438 suitable for cases where survey data exists in order to further develop the understanding of
439 recent, current and future channel network evolution in coastal systems worldwide.

440 **4.3 Implications**

441 This study facilitates a comparison between the historic discharge annexation of the Mississippi-
442 Atchafalaya System to current understanding of general avulsion controls. The super-elevation of
443 the Mississippi River at Red River Landing was small, although consistent with prevailing
444 models. Water surface elevation peaked at 16 m MSL during large floods prior to annexation,
445 and was 9 m MSL for average flows (Fig. 5b,d). Compared to the minimum channel bed
446 elevation (-11 m MSL) and minimum floodplain elevation in the region (8 m MSL; Aslan et al.
447 2005), the fraction of flow depth above the flood plain (the superelevation ratio) was 0.05 - 0.3.
448 This value is consistent with the superelevation ratios estimated for the avulsion that produced
449 Bayou Lafourche (~0.1; Törnqvist & Bridge, 2002) and laboratory experiments (0.3; Ganti et al.,
450 2016).

451 We also find it remarkable that the lower Mississippi River was slightly erosional (Figure 5d)
452 during the pivotal 24 year period of discharge increase (Figure 2). This contrasts with prevailing
453 models which expect deposition in the main channel before and during avulsion to drive the flow
454 reorganization into the new channel (Ganti et al., 2016). Rather than the “choking” of the main
455 channel, the key control on discharge increase shown was the enlargement of the upper
456 Atchafalaya River, consistent with an incisional avulsion model (Hajek & Edmonds, 2014;

457 Slingerland & Smith, 2004), where the excavation of the new channel is of primary importance.
458 The sandy, easily erodible deposits found in the upper Atchafalaya River region (Aslan et al.,
459 2005), the dredging at Old River between 1878 and 1937 (Mossa, 2013), and the dredging of the
460 Atchafalaya River between 1932 and 1951 (R_{pre_D}) may have assisted the natural erosion
461 observed in the upper Atchafalaya River.

462 Analyses of backwater flow (eq. 3) with smoothly varying bed topography show that channel
463 bed erosion or deposition results in changes to the flow field that propagate upstream. Such
464 changes decay asymptotically and scale with the backwater length scale (Chadwick et al., 2019;
465 Ribberink & Van Der Sande, 1985); roughly 500 km in the case of the Mississippi Delta
466 (Chatanantavet et al., 2012). The stage reduction at RRL due to erosion in the Mississippi River
467 up to 300 km downstream is an example of this (Figure 5b). However, the growth of lacustrine
468 deltas in Grand Lake just 148-180 km downstream of Red River Landing did not factor into
469 discharge partitioning or stage change there. While these deltas did act to reduce channel cross
470 sectional area and increase stage in R_{pre_GL} by 0.8 m relative to R_{pre} within the delta area
471 (Figure 6a), the water surfaces of the R_{pre} and R_{pre_GL} collapsed on one another in the lower
472 Atchafalaya River and were similar at all points above. The steep water surface slopes (locally -
473 6.3×10^{-4}) associated with the M2 curve in the lower Atchafalaya River overwhelmed gradual
474 trends stemming from non-uniform backwater flow.

475 Our work has important implications for management of the Mississippi-Atchafalaya system,
476 and for flow management in complex networks in general. The Old River Control Structure
477 currently regulates discharge partitioning in the system. However, stress on this regulation has
478 occurred in the past, notably in 1973 when the Low Sill structure was damaged during a large
479 flood (Mossa, 2016), and evolution of the channel network could impart additional stress. Large-
480 scale coastal restoration efforts are being undertaken to make coastal Louisiana resilient to
481 hazardous changes in the coming century (Bentley et al., 2016; CPRA, 2017; Gasparini & Yuill,
482 2020). These plans may benefit from optimizing f_A to the wide range of restoration objectives
483 (e.g. Kenney et al., 2013; Peyronnin et al., 2017).

484
485 For the management of flow through complex networks in general, our work stresses several
486 things. First (and most intuitively), changes closer to a channel branch, such as the natural
487 erosion of the upper Atchafalaya River, affect the hydrodynamics at a bifurcation more
488 significantly. Second, small changes to the largest channels of the system can significantly affect
489 the smaller channels in the network. The changes to the lower Mississippi River acted to reduce
490 stage at RRL, and could have potentially reduced f_A , had the Atchafalaya Basin not evolved.
491 Third, this study shows that reaches like the lower Atchafalaya River - which have relatively
492 small channels, steep water surface slopes, and naturally produce an M2 curve under non-flood
493 discharges - can act as a “choke point” in the system. Increased connectivity caused by dredging
494 across these reaches will reduce stage and increase shear stress upstream. Finally, apparently
495 large changes downstream of these reaches (such as delta deposition) may not be propagated
496 upstream in a significant way.

497 **5 Conclusions**

498 We present evidence that the rapid increase in water discharge into the Atchafalaya River
499 between 1926 and 1950 can be attributed to three important natural and human-influenced

500 changes to the Mississippi-Atchafalaya system over that period. First, the relatively consistent
 501 natural erosion of the upper Atchafalaya River produced significant increases in the fraction of
 502 water discharge entering the Atchafalaya River, as was originally interpreted by the US Army
 503 Corps of Engineers (Fisk, 1952). Second, significant channel dredging in the lower Atchafalaya
 504 River further increased partitioning by increasing connectivity through a steep reach, potentially
 505 increasing shear stresses in the eroding channel upstream. Third, the subtle erosion of the lower
 506 Mississippi River acted to reduce stage at Red River Landing, and reduce partitioning to the
 507 Atchafalaya River. Finally, the extensive lacustrine deltas that formed in the lower Atchafalaya
 508 Basin did not significantly influence partitioning. These results demonstrate the natural and
 509 anthropogenic forcings on a large complex channel network can be isolated and quantitatively
 510 evaluated in a manner that can aid in attribution and delta management.

511 **Acknowledgments, Samples, and Data**

512 This research project was conceived by J.S. Data digitization was performed by G.M. and K. M.,
 513 with additional help from Micheal Amos and J.S. Important methodological updates were
 514 provided by H.M. Final modeling analyses were performed primarily by J.S., with important
 515 contributions by K.M. and G.M., a preliminary version of this work was published as an M.S.
 516 thesis by McCain (2016). All authors contributed to writing, with primary contributions by J.S.
 517 Data and MATLAB code required to reproduce this study is available at
 518 <https://doi.org/10.6084/m9.figshare.12440279.v3>, and dataset available at
 519 <https://doi.org/10.6084/m9.figshare.13645601.v1>. Support was provided by the DOE under
 520 DESC0016163 to JS. The authors declare no real or perceived financial interests in this study.
 521 We thank Drs. Rebecca Caldwell, Enrica Viparelli and two anonymous reviewers for thorough
 522 and constructive reviews. This work is dedicated to the late Dennis Trombatore, Geology
 523 Librarian at University of Texas, who made the original USACE reports available to J.S. in
 524 2009.

525 **Appendix: Notation**

526	A	Cross-sectional Area of a channel below the water surface (L^2)
527	A.R.	Atchafalaya River
528	M.R.	Mississippi River
529	C_f	Dimensionless friction factor (-)
530	CSA	Bankfull cross-sectional area of transects, measured by USACE (L^2)
531	E	Error function for optimization (L^2)
532	F	Froude number (-)
533	f_i	Fraction of upstream flow entering channel reach i
534	f_A	Fraction of Q_0 entering the Atchafalaya River.
535	g	Gravitational acceleration (L/T^2)
536	Γ	Wetted perimeter at a cross section; A divided by the wetted surface width (L)
537	η	minimum bed elevation, thalweg elevation (L relative to mean sea level; MSL)
538	Q	Discharge (L^3/T)
539	Q_0	Input water discharge upstream of Red River Landing (L^3/T)
540	S	Bed slope ($-\partial\eta/\partial x$; -)
541	S_f	Frictional slope (-)
542	t	Time (T)
543	u	Water velocity, averaged across A (L/T)
544	x	Downstream coordinate (L)
545	z	Water surface elevation (L relative to mean sea level; MSL)

546

547 **References**

- 548 Aslan, A., Autin, W. J., & Blum, M. D. (2005). Causes of river avulsion: insights from the late Holocene avulsion
549 history of the Mississippi River, USA. *Journal of Sedimentary Research*, 75(4), 650–664.
- 550 Bain, R. L., Hale, R. P., & Goodbred, S. L. (2019). Flow Reorganization in an Anthropogenically Modified Tidal
551 Channel Network: An Example from the Southwestern Ganges-Brahmaputra-Meghna Delta. *Journal of*
552 *Geophysical Research: Earth Surface*, 0(ja). <https://doi.org/10.1029/2018JF004996>
- 553 Bentley, S. J., Blum, M. D., Maloney, J., Pond, L., & Paulsell, R. (2016). The Mississippi River source-to-sink
554 system: Perspectives on tectonic, climatic, and anthropogenic influences, Miocene to Anthropocene. *Earth-*
555 *Science Reviews*, 153, 139–174. <https://doi.org/10.1016/j.earscirev.2015.11.001>
- 556 Bhattacharya, J. P., Miall, A. D., Ferron, C., Gabriel, J., Randazzo, N., Kynaston, D., et al. (2019). Time-
557 stratigraphy in point sourced river deltas: Application to sediment budgets, shelf construction, and paleo-
558 storm records. *Earth-Science Reviews*, 199, 102985. <https://doi.org/10.1016/j.earscirev.2019.102985>
- 559 Biedenharn, D. S., & Watson, C. C. (1997). Stage adjustment in the Lower Mississippi River, USA. *Regulated*
560 *Rivers: Research & Management*, 13(6), 517–536. [https://doi.org/10.1002/\(SICI\)1099-](https://doi.org/10.1002/(SICI)1099-1646(199711/12)13:6<517::AID-RRR482>3.0.CO;2-2)
561 [1646\(199711/12\)13:6<517::AID-RRR482>3.0.CO;2-2](https://doi.org/10.1002/(SICI)1099-1646(199711/12)13:6<517::AID-RRR482>3.0.CO;2-2)
- 562 Blum, M. D. (2019). Organization and reorganization of drainage and sediment routing through time: the
563 Mississippi River system. *Geological Society, London, Special Publications*, 488.
564 <https://doi.org/10.1144/SP488-2018-166>
- 565 Blum, M. D., & Roberts, H. H. (2012). The Mississippi Delta Region: Past, Present, and Future. *Annual Review of*
566 *Earth and Planetary Sciences*, 40(1), 655–683. <https://doi.org/10.1146/annurev-earth-042711-105248>
- 567 Buschman, F. A., Hoitink, A. J. F., Van der Vegt, M., & Hoekstra, P. (2010). Subtidal flow division at a shallow
568 tidal junction. *Water Resources Research*, 46, W12515-1.
- 569 Chadwick, A. J., Lamb, M. P., Moodie, A. J., Parker, G., & Nittrouer, J. A. (2019). Origin of a Preferential Avulsion
570 Node on Lowland River Deltas. *Geophysical Research Letters*, 46(8), 4267–4277.
571 <https://doi.org/10.1029/2019GL082491>
- 572 Chatanantavet, P., Lamb, M. P., & Nittrouer, J. A. (2012). Backwater controls of avulsion location on deltas.
573 *Geophysical Research Letters*, 39(1), n/a-n/a. <https://doi.org/10.1029/2011GL050197>
- 574 Chow, V. T. (1959). Open-channel hydraulics.

- 575 CPRA. (2017). *Louisiana's Comprehensive Master Plan for a Sustainable Coast*. Baton Rouge, LA: State of
576 Louisiana. Retrieved from <http://coastal.la.gov/our-plan/>
- 577 Edmonds, D. A. (2012). Stability of backwater-influenced river bifurcations: A study of the Mississippi-Atchafalaya
578 system. *Geophysical Research Letters*, *39*(8), n/a-n/a. <https://doi.org/10.1029/2012GL051125>
- 579 Engelund, F., & Hansen, E. (1967). *A Monograph on Sediment Transport in Alluvial Streams*. Copenhagen: Teknik
580 Forlag.
- 581 Fisk, H. N. (1952). *Geological investigation of the Atchafalaya Basin and the problem of Mississippi River*
582 *diversion*. Vicksburg, Mississippi: U.S. Corps of Engineers, Mississippi River Commission.
- 583 Galler, J. J., Bianchi, T. S., Alison, M. A., Wysocki, L. A., Campanella, R., Narasimhan, T. N., et al. (2003).
584 Biogeochemical implications of levee confinement in the lowermost Mississippi River. *EOS [American*
585 *Geophysical Union Transactions]*, *84*(44), 469–484.
- 586 Ganti, V., Chu, Z., Lamb, M. P., Nittrouer, J. A., & Parker, G. (2014). Testing morphodynamic controls on the
587 location and frequency of river avulsions on fans versus deltas: Huanghe (Yellow River), China.
588 *Geophysical Research Letters*, *41*(22), 2014GL061918. <https://doi.org/10.1002/2014GL061918>
- 589 Ganti, V., Chadwick, A. J., Hassenruck-Gudipati, H. J., & Lamb, M. P. (2016). Avulsion cycles and their
590 stratigraphic signature on an experimental backwater-controlled delta. *Journal of Geophysical Research:*
591 *Earth Surface*, *121*(9), 1651–1675. <https://doi.org/10.1002/2016JF003915>
- 592 Gasparini, N., & Yuill, B. T. (2020). High Water: Prolonged Flooding on the Deltaic Mississippi River. Retrieved
593 May 19, 2020, from <https://eos.org/features/high-water-prolonged-flooding-on-the-deltaic-mississippi-river>
- 594 Hajek, E. A., & Edmonds, D. A. (2014). Is river avulsion style controlled by floodplain morphodynamics? *Geology*,
595 *42*(3), 199–202. <https://doi.org/10.1130/G35045.1>
- 596 Hoitink, A. J. F., Nittrouer, J. A., Passalacqua, P., Shaw, J. B., Langendoen, E. J., Huismans, Y., & Maren, D. S.
597 van. (2020). Resilience of river deltas in the Anthropocene. *Journal of Geophysical Research: Earth*
598 *Surface*, e2019JF005201. <https://doi.org/10.1029/2019JF005201>
- 599 Kafadar, K. (2014). Notched Box-And-Whisker Plot. In *Wiley StatsRef: Statistics Reference Online*. American
600 Cancer Society. <https://doi.org/10.1002/9781118445112.stat00467>
- 601 Karim, F. (1995). Bed Configuration and Hydraulic Resistance in Alluvial-Channel Flows. *Journal of Hydraulic*
602 *Engineering*, *121*(1), 15–25. [https://doi.org/10.1061/\(ASCE\)0733-9429\(1995\)121:1\(15\)](https://doi.org/10.1061/(ASCE)0733-9429(1995)121:1(15))

- 603 Kästner, K., Hoitink, A. J. F., Vermeulen, B., Geertsema, T. J., & Ningsih, N. S. (2017). Distributary channels in the
604 fluvial to tidal transition zone. *Journal of Geophysical Research: Earth Surface*, *122*(3), 696–710.
605 <https://doi.org/10.1002/2016JF004075>
- 606 Kenney, M. A., Hobbs, B. F., Mohrig, D., Huang, H., Nittrouer, J. A., Kim, W., & Parker, G. (2013). Cost analysis
607 of water and sediment diversions to optimize land building in the Mississippi river delta. *Water Resources*
608 *Research*. <https://doi.org/10.1002/wrcr.20139>
- 609 Kesel, R. H. (2003). Human modifications to the sediment regime of the Lower Mississippi River flood plain.
610 *Geomorphology*, *56*(3), 325–334. [https://doi.org/10.1016/S0169-555X\(03\)00159-4](https://doi.org/10.1016/S0169-555X(03)00159-4)
- 611 Kleinhans, M. G., Cohen, K. M., Hoekstra, J., & IJmker, J. M. (2011). Evolution of a bifurcation in a meandering
612 river with adjustable channel widths, Rhine delta apex. *Earth Surface Processes and Landforms*, *36*(15),
613 2011–2027. <https://doi.org/10.1002/esp.2222>
- 614 Kleinhans, M. G., de Haas, T., Lavooi, E., & Makaske, B. (2012). Evaluating competing hypotheses for the origin
615 and dynamics of river anastomosis. *Earth Surface Processes and Landforms*, *37*(12), 1337–1351.
616 <https://doi.org/10.1002/esp.3282>
- 617 Kleinhans, M. G., Ferguson, R. I., Lane, S. N., & Hardy, R. J. (2012). Splitting rivers at their seams: bifurcations
618 and avulsion. *Earth Surface Processes and Landforms*. <https://doi.org/10.1002/esp.3268>
- 619 Knights, D., Sawyer, A. H., Barnes, R. T., Piliouras, A., Schwenk, J., Edmonds, D. A., & Brown, A. M. (2020).
620 Nitrate Removal Across Ecogeomorphic Zones in Wax Lake Delta, Louisiana (USA). *Water Resources*
621 *Research*, *56*(8), e2019WR026867. <https://doi.org/10.1029/2019WR026867>
- 622 Knox, R. L., & Latrubesse, E. M. (2016). A geomorphic approach to the analysis of bedload and bed morphology of
623 the Lower Mississippi River near the Old River Control Structure. *Geomorphology*, *268*, 35–47.
624 <https://doi.org/10.1016/j.geomorph.2016.05.034>
- 625 Lamb, M. P., Nittrouer, J. A., Mohrig, D., & Shaw, J. B. (2012). Backwater and river plume controls on scour
626 upstream of river mouths: Implications for fluvio-deltaic morphodynamics. *Journal of Geophysical*
627 *Research*, *117*(F1), F01002. <https://doi.org/10.1029/2011JF002079>
- 628 Latimer, R. A., & Schweitzer, C. W. (1951). *The Atchafalaya River study: A report based engineering and*
629 *geological studies of the enlargement of Old and Atchafalaya Rivers* (Vol. 1,2,3). Vicksburg, Mississippi:
630 U.S. Army Corps of Engineers, Mississippi River Commission.

- 631 Lazarus, E. D., & Goldstein, E. B. (2019). Is There a Bulldozer in your Model? *Journal of Geophysical Research:*
632 *Earth Surface*, 124(3), 696–699. <https://doi.org/10.1029/2018JF004957>
- 633 Martin, J., Sheets, B., Paola, C., & Hoyal, D. (2009). Influence of steady base-level rise on channel mobility,
634 shoreline migration, and scaling properties of a cohesive experimental delta. *Journal of*
635 *Geophysical Research*, 114, 15 PP. <https://doi.org/200910.1029/2008JF001142>
- 636 McCain, G. (2016). Influences of Channel Dredging on Avulsion Potential at the Atchafalaya River. *Theses and*
637 *Dissertations*. Retrieved from <https://scholarworks.uark.edu/etd/1559>
- 638 McPhee, J. (1987, February 16). Atchafalaya. Retrieved from
639 <https://www.newyorker.com/magazine/1987/02/23/atchafalaya>
- 640 Mossa, J. (2013). Historical changes of a major juncture: Lower Old River, Louisiana. *Physical Geography*, 34(4–
641 05), 315–334. <https://doi.org/10.1080/02723646.2013.847314>
- 642 Mossa, J. (2016). The changing geomorphology of the Atchafalaya River, Louisiana: A historical perspective.
643 *Geomorphology*, 252, 112–127. <https://doi.org/10.1016/j.geomorph.2015.08.018>
- 644 Nittrouer, J. A., Shaw, J. B., Lamb, M. P., & Mohrig, D. (2012). Spatial and temporal trends for water-flow velocity
645 and bed-material transport in the lower Mississippi River. *Geol. Soc. Am. Bull*, 124, 400–414.
646 <https://doi.org/10.1130/B30497.1>
- 647 Parker, G. (2004). *1D Sediment Transport Morphodynamics with applications to Rivers and Turbidity Currents*.
648 Retrieved from [http://hydrolab.illinois.edu/people/parkerg/morphodynamics_e-](http://hydrolab.illinois.edu/people/parkerg/morphodynamics_e-book.htm?q=people/parkerg/morphodynamics_e-book.htm)
649 [book.htm?q=people/parkerg/morphodynamics_e-book.htm](http://hydrolab.illinois.edu/people/parkerg/morphodynamics_e-book.htm)
- 650 Peyronnin, N. S., Caffey, R. H., Cowan, J. H., Justic, D., Kolker, A. S., Laska, S. B., et al. (2017). Optimizing
651 Sediment Diversion Operations: Working Group Recommendations for Integrating Complex Ecological
652 and Social Landscape Interactions. *Water*, 9(6), 368. <https://doi.org/10.3390/w9060368>
- 653 Ribberink, J. S., & Van Der Sande, J. T. M. (1985). Aggradation in rivers due to overloading - analytical
654 approaches. *Journal of Hydraulic Research*, 23(3), 273–283. <https://doi.org/10.1080/00221688509499355>
- 655 Roberts, H., Adams, R., & Cunningham, R. (1980). Evolution of sand-dominant subaerial phase, Atchafalaya Delta,
656 Louisiana. *American Association of Petroleum Geologists Bulletin*, 64, 264–279.

- 657 Sanks, K. M., Shaw, J. B., & Naithani, K. (2020). Field-based Estimate of the Sediment Deficit in Coastal
658 Louisiana. *Journal of Geophysical Research: Earth Surface*, e2019JF005389.
659 <https://doi.org/10.1029/2019JF005389>
- 660 Saucier, R. T. (1994). *Geomorphology and Quarternary Geologic History of the Lower Mississippi Valley. Volume*
661 *2*. DTIC Document. Retrieved from
662 <http://oai.dtic.mil/oai/oai?verb=getRecord&metadataPrefix=html&identifier=ADA299155>
- 663 Shanno, D. F. (1970). Conditioning of quasi-Newton methods for function minimization. *Mathematics of*
664 *Computation*, 24(111), 647–656.
- 665 Slingerland, R., & Smith, N. D. (1998). Necessary conditions for a meandering-river avulsion. *Geology*, 26(5), 435–
666 438. [https://doi.org/10.1130/0091-7613\(1998\)026<0435:NCFAMR>2.3.CO;2](https://doi.org/10.1130/0091-7613(1998)026<0435:NCFAMR>2.3.CO;2)
- 667 Slingerland, R., & Smith, N. D. (2004). River avulsions and their deposits. *Annu. Rev. Earth Planet. Sci.*, 32, 257–
668 285.
- 669 Smith, L. M., & Winkley, B. R. (1996). The response of the Lower Mississippi River to river engineering.
670 *Engineering Geology*, 45(1), 433–455. [https://doi.org/10.1016/S0013-7952\(96\)00025-7](https://doi.org/10.1016/S0013-7952(96)00025-7)
- 671 Syvitski, J. P. M. (2008). Deltas at risk. *Sustainability Science*, 3(1), 23–32. [https://doi.org/10.1007/s11625-008-](https://doi.org/10.1007/s11625-008-0043-3)
672 [0043-3](https://doi.org/10.1007/s11625-008-0043-3)
- 673 Tessler, Z. D., Vörösmarty, C. J., Grossberg, M., Gladkova, I., Aizenman, H., Syvitski, J. P. M., & Foufoula-
674 Georgiou, E. (2015). Profiling risk and sustainability in coastal deltas of the world. *Science*, 349(6248),
675 638–643. <https://doi.org/10.1126/science.aab3574>
- 676 Törnqvist, T. E., & Bridge, J. S. (2002). Spatial variation of overbank aggradation rate and its influence on avulsion
677 frequency. *Sedimentology*, 49(5), 891–905.
- 678 Tye, R. S., & Coleman, J. M. (1989). Evolution of Atchafalaya lacustrine deltas, south-central Louisiana.
679 *Sedimentary Geology*, 65(1), 95–112. [https://doi.org/10.1016/0037-0738\(89\)90008-0](https://doi.org/10.1016/0037-0738(89)90008-0)
- 680 USACE. (1915). *1913 Mississippi River Hydrographic Survey*. Retrieved from
681 [https://www.mvn.usace.army.mil/Missions/Engineering/Geospatial-](https://www.mvn.usace.army.mil/Missions/Engineering/Geospatial-Section/MRHB_Historic/MRHB_1913/)
682 [Section/MRHB_Historic/MRHB_1913/](https://www.mvn.usace.army.mil/Missions/Engineering/Geospatial-Section/MRHB_Historic/MRHB_1913/)

- 683 USACE. (1950). *1949 Mississippi River Hydrographic Survey*. Retrieved from
684 [https://www.mvn.usace.army.mil/Missions/Engineering/Geospatial-](https://www.mvn.usace.army.mil/Missions/Engineering/Geospatial-Section/MRHB_Historic/MRHB_1913/)
685 [Section/MRHB_Historic/MRHB_1913/](https://www.mvn.usace.army.mil/Missions/Engineering/Geospatial-Section/MRHB_Historic/MRHB_1913/)
- 686 Vinh, V. D., Ouillon, S., Thanh, T. D., & Chu, L. V. (2014). Impact of the Hoa Binh dam (Vietnam) on water and
687 sediment budgets in the Red River basin and delta. *Hydrology and Earth System Sciences*, *18*(10), 3987–
688 4005. <https://doi.org/10.5194/hess-18-3987-2014>
- 689 Viparelli, E., Nittrouer, J. A., & Parker, G. (2015). Modeling flow and sediment transport dynamics in the
690 lowermost Mississippi River, Louisiana, USA, with an upstream alluvial-bedrock transition and a
691 downstream bedrock-alluvial transition: Implications for land building using engineered diversions.
692 *Journal of Geophysical Research: Earth Surface*, *120*(3), 534–563. <https://doi.org/10.1002/2014JF003257>
- 693 Wang, B., & Xu, Y. J. (2016). Long-term geomorphic response to flow regulation in a 10-km reach downstream of
694 the Mississippi–Atchafalaya River diversion. *Journal of Hydrology: Regional Studies*, *8*, 10–25.
695 <https://doi.org/10.1016/j.ejrh.2016.08.002>
- 696 Wang, B., & Xu, Y. J. (2018). Decadal-Scale Riverbed Deformation and Sand Budget of the Last 500 km of the
697 Mississippi River: Insights Into Natural and River Engineering Effects on a Large Alluvial River. *Journal*
698 *of Geophysical Research: Earth Surface*, *123*(5), 874–890. <https://doi.org/10.1029/2017JF004542>
- 699 Wang, Z. B., De Vries, M., Fokink, R. J., & Langerak, A. (1995). Stability of river bifurcations in ID
700 morphodynamic models. *Journal of Hydraulic Research*, *33*(6), 739–750.
- 701 Wilson, C., Goodbred, S., Small, C., Gilligan, J., Sams, S., Mallick, B., & Hale, R. (2017). Widespread infilling of
702 tidal channels and navigable waterways in human-modified tidal delta plain of southwest Bangladesh. *Elem*
703 *Sci Anth*, *5*(0). <https://doi.org/10.1525/elementa.263>
- 704 Wu, C.-Y., & Mossa, J. (2019). Decadal-Scale Variations of Thalweg Morphology and Riffle–Pool Sequences in
705 Response to Flow Regulation in the Lowermost Mississippi River. *Water*, *11*(6), 1175.
706 <https://doi.org/10.3390/w11061175>

707

708

709